The Mechanism of the Hydrogenation of Cyclohexene and Benzene on Nickel–Tungsten Sulfide Catalysts

R. J. H. VOORHOEVE* AND J. C. M. STUIVER

Koninklijke/Shell-Laboratorium, Amsterdam, The Netherlands

Hydrogenation of cyclohexene and benzene on nickel–tungsten sulfide and tungsten disulfide are compared. The hydrogenation activity of these catalysts had been attributed to tungsten ions in the surface of WS_2 crystallites. Comparison of catalysts with and without nickel corroborates this. The role of nickel in multiplying the number of active tungsten sites is evaluated. Possible adsorption mechanisms for cyclohexene and benzene on such sites are discussed. Differences between the hydrogenation of benzene and cyclohexene, as well as the effect of nickel, are explained on the basis of a discussion of the nature of the active sites.

1. INTRODUCTION

In the two foregoing papers (1, 2), the kinetics of the hydrogenation of cyclohexene and benzene on supported and bulk nickel–tungsten sulfide catalysts have been presented. A relation between the benzene rate constant and the number of W^{3+} ions in the surface has been established. It was also shown that bulk and supported catalysts contain the same active sites, which were identified as anion-vacancies. Differences between benzene and cyclohexene hydrogenation sites were demonstrated.

In the present report it is shown that not only benzene, but also cyclohexene is hydrogenated on tungsten sites. The earlier assignment for benzene hydrogenation sites is further substantiated. Structural and catalytic effects of nickel are singled out by comparison of sulfide catalysts with and without nickel. These effects are discussed in relation with the structure of adsorption complexes for benzene and cyclohexene.

2. EXPERIMENTAL METHODS

Benzene and cyclohexene were hydrogenated in a fixed-bed microflow reactor.

* Present address: Bell Telephone Laboratories, Incorporated, Murray Hill, New Jersey 07974.

Generally 1% v CS_2 was added to the liquid feed to prevent reduction of the sulfide catalyst used. Details of the kinetic measurement procedure and of the mathematical analysis of the data were given earlier, together with particulars about chemicals used, preparation methods of catalysts and analytical procedures (1). Relevant details about catalysts used in the present work are collected in Table 1. X-Ray analyses were made with a Debeye Scherrer camera (Philips PW 1024/10) and with instruments also used in our earlier work (3). Copper $K\alpha$ radiation was applied throughout. For microscopic observation samples of sulfide were embedded in Bakelite molds and wet-polished with alumina powder. The microscope was a Reichert MeF.

3. HYDROGENATION ACTIVITIES OF WS_2 AND Ni–W–S CATALYSTS

Two test reactions are employed to study the properties of these catalysts, namely the hydrogenations of benzene and of cyclohexene. Cyclohexene has been hydrogenated over a variety of bulk and alumina-supported tungsten-disulfide based catalysts and over nickel subsulfide Ni_3S_2. The kinetics of the conversion over tungsten disulfide, WS_2, is found to be the same as over nickel–

TABLE 1
PREPARATION AND PROPERTIES OF CATALYSTS USED

No.	Composition[a]	Preparation	Specific surface area (m^2/g)	Activity[b] k [ml(g cat)$^{-1}$ hr^{-1} atm^{-1}]	Temp (°C)
1	$Ni_{0.5}WS_x$	WS_2 + Ni, 800°C	0.80	B 0.16	400
2	WS_2	Elements, 850°C	2.50	C 0.166	286
				B 0.00065	400
3	Ni_3S_2	Elements, 700°C	0.17		
4	Ni_3S_2 + 6 WS_2	Mixture of (2) + (3)	2.17		
5	$Ni_{0.5}WS_x$	WS_2 + Ni, 800°C	1.00	C 0.96	286
6	$Ni_{0.53}WS_x/Al_2O_3$	Impregnation, calcination, and sulfiding	143	C 5.7[c]	265
	32.5% w Ni-W-S	(BASF 8376)			
7	WS_x/Al_2O_3 30.5% w WS_2	Impregnation, calcination, and sulfiding		C 0.40	265
8	Ni_yWS_x	Elements, 800°C	—[d]		
9	$Ni_{0.016}WS_2$	Impregnated WS_2	2.20		

[a] The sulfur content of the catalysts is dependent on the H_2S/H_2 ratio and the temperature during equilibration. The x indicates that it is not known precisely, but $x \simeq$ 2.0–2.3.

[b] First order rate constant at the temperature given in the next column, 1% v CS_2 admixed with the hydrocarbon, which is either benzene (B); or cyclohexene (C). Total pressure 48 atm.

[c] Taken from curve I, Fig. 4, Ref. (1).

[d] Specific surface area dependent on nickel content y.

tungsten sulfide: the reaction is first order in cyclohexene and is inhibited by carbon disulfide. Rate constants were calculated from the experimental data by applying the kinetic analysis given before (1).

The conversion of carbon disulfide over WS_2 is quite slow, with a zero order rate constant of circa 5×10^{-3} ml CS_2/hr/m^2 catalyst surface, and independent of the temperature. In fact there is some question whether this conversion is not due to the preheater.

The rate constants found for cyclohexene over bulk catalysts are given in Fig. 1. Curves drawn in Fig. 1 are best fits of the temperature-dependent activation energies determined before [Fig. 6 in Ref. (1)] to the experimental data points. The constant vertical distance between the rates over WS_2 and Ni–W–S indicates that the hydrogenation process on both catalysts is characterized by the same temperature-dependent activation energy. Nickel appears to increase the number of active sites without changing their intrinsic activity. Hydrogenation over Ni_3S_2 is shown to be much slower than over
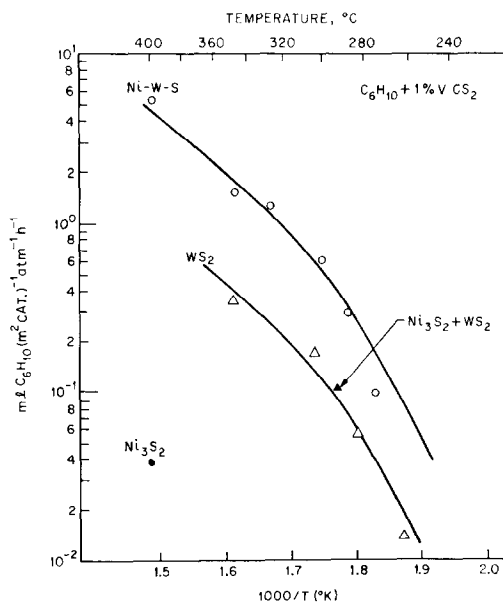

FIG. 1. Hydrogenation rate constants for cyclohexene on bulk catalysts: (○) nickel–tungsten sulfide; (△) tungsten disulfide; (●) nickel subsulfide; (▲) a mechanical mixture of Ni_3S_2 and WS_2 (catalysts Nos. 1, 2, 3, and 4, respectively, in Table 1).

either WS_2 or Ni–W–S. A mechanical mixture of Ni_3S_2 and WS_2 behaved very much like WS_2. This shows that the synergic effect of the two metals is not due to mere mechanical proximity of the two sulfides.

From Fig. 1, the effect of nickel seems to be an increase in the activity for cyclohexene conversion by about a factor 5. This ratio is dependent, however, on the specific surface area of bulk nickel–tungsten sulfide, as $Ni_{0.5}WS_2$ has been found to show a mechano-chemical effect. The specific activity (rate constant per unit catalyst surface area) is affected by grinding the catalyst in a ball mill. It rises to a maximum at 1 m^2/g specific surface area and then decreases again. This effect is quite reproducible, but its cause unknown.* Comparing WS_2 (No. 2, Table 1) with the most active $Ni_{0.5}WS_2$ of 1 m^2/g (No. 5, Table 1) yields a factor of 15 for the increase in the activity per square meter brought about by nickel. A similar comparison of the hydrogenation of cyclohexene over WS_2 and $Ni_{0.5}WS_2$, both supported on alumina, shows nickel to raise the activity by a factor of about 15 (compare Nos. 6 and 7 in Table 1).

The effect of nickel is further investigated by varying its amount in the Ni–W–S catalyst. A number of unsupported catalysts with different Ni/W atomic ratios were prepared in an identical manner (No. 8, Table 1). Their activities in the hydrogenation of cyclohexene at 286°C are shown in Fig. 2. A relatively small amount of nickel appears to bring about most of the beneficial effect and beyond $Ni/(Ni + W) \sim 0.1$ there is even some decline in activity.

Focusing now on the hydrogenation of benzene to cyclohexane as test reaction in the study of the effect of nickel on tungsten-disulfide based catalysts, we find rather similar effects as with cyclohexene, but also note some significant differences. First alumina-supported catalysts, viz., WS_2 and Ni–W–S (Nos. 6 and 7, Table 1) are compared. Figure 3 shows the measured first order hydrogenation rate constants versus reciprocal temperature. The apparent acti-

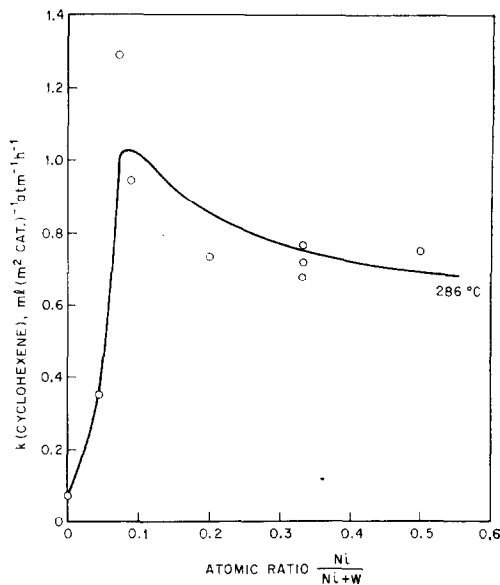* The effect is found in hydrogenation of cyclohexene, but not of benzene.

FIG. 2. Effect of the Ni/W atomic ratio in Ni–W–S catalysts on the hydrogenation rate of cyclohexene (Catalyst No. 8, Table 1).
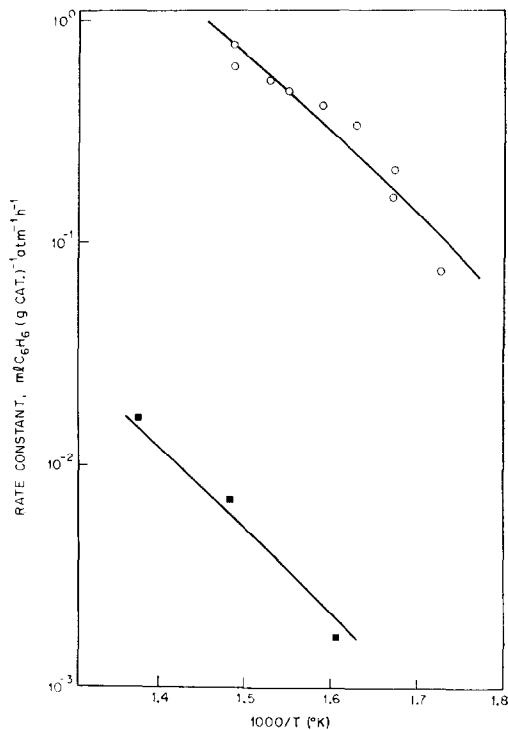

FIG. 3. Hydrogenation rate constants for benzene on alumina-supported tungsten-disulfide based catalysts: (○) $Ni_{0.53}WS_x$; (■) WS_x (Nos. 6 and 7, Table 1).

vation energies for these catalysts do not differ significantly and equal about 17 kcal/mole. Although these rather limited results are, in itself, not sufficient proof that the active sites for benzene hydrogenation in both types of catalyst are the same tungsten sites, they corroborate that conclusion, which was drawn from correlation of kinetic data with ESR results (2). The activity of $Ni_{0.5}WS_2$ is about 200 times that of WS_2 for these supported catalysts, a significantly higher ratio than found for cyclohexene over these same catalysts. Comparing now bulk WS_2 and $Ni_{0.5}WS_2$ in the benzene reaction yields a factor 250 for the activity increase effected by nickel (compare Nos. 1 and 2 in Table 1). It was further established that in benzene hydrogenation, as in cyclohexene conversion, the first small amounts of nickel count most (Table 2).

4. STRUCTURAL EFFECTS OF NICKEL ON WS_2

Tungsten disulfide has the trigonal-prismatic MoS_2-type structure (4), characterized by S–W–S sandwich layers stacked in such a way that empty close-packed sulfur double layers are formed (Fig. 4). The sandwiches are held together by Van

TABLE 2

EFFECT OF THE Ni/W ATOMIC RATIO IN Ni–W–S CATALYSTS ON THE HYDROGENATION ACTIVITY FOR BENZENE

Catalyst no. (Table 1)	Ni/W atomic ratio	Specific activity[a] [ml(m² cat)$^{-1}$ hr^{-1} atm^{-1}]
2	0	0.00065
9	0.016	0.031
1	0.5	0.16

[a] At 400°C, 1% v CS_2 in benzene, 48 atm total pressure.

der Waals forces only. The same weak bonding is presumably responsible for the fact that alkali metal intercalation compounds with alkali ions randomly distributed in the holes of the sulfur double layer are easily formed at liquid-ammonia temperature (5). Niobium disulfide and tantalum disulfide, with a trigonal-prismatic layer structure which is only slightly different from the WS_2 structure (6), accomodate nickel and other first-row transition metals in sulfur octahedrons between the sandwich layers, forming a superstructure (7). In MoS_2, cobalt may even be incorporated under the formation of a new structure
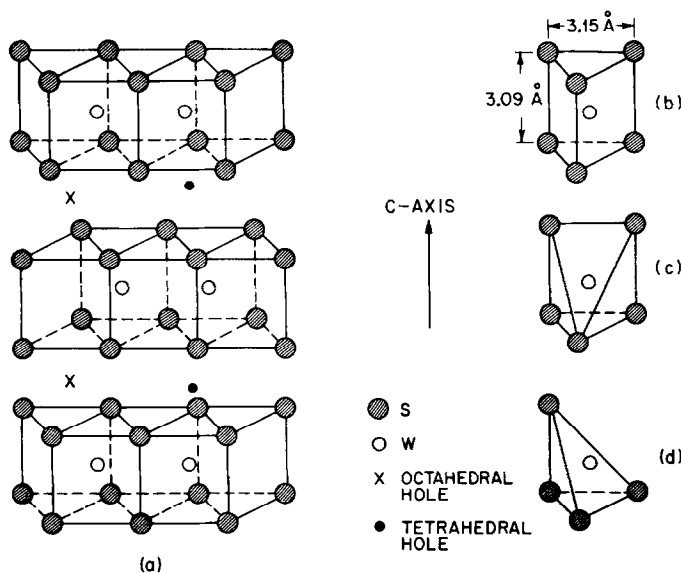

FIG. 4. The structure of tungsten disulfide: (a) the stacking of layers illustrating the position of octahedral holes which may be partly occupied by nickel; (b) the site symmetry of tungsten ions in the bulk; (c) same for a sideface; (d) same for an edge parallel to the c-axis.

with both cobalt and molybdenum in octahedral holes (8). So, although X-ray analysis of nickel–tungsten sulfide catalysts has not revealed any new ternary compound in addition to WS_2 and Ni_3S_2, it is entirely conceivable that nickel would form a solid solution in the WS_2 sandwich structure. This would not be expected to affect the lattice parameters of WS_2, as incorporation of nickel did not change the parameters of TaS_2 either (7). Evidence for insertion of nickel in WS_2 found by X-ray analysis and optical microscopy is presented below.

Unsupported tungsten disulfide samples containing various amounts of nickel, but all prepared from the elements at 800°C in an identical procedure were studied with a Guinier camera. Densitometer traces of the diffraction patterns (Fig. 5) show that nickel improves the crystallinity of the WS_2 struc-

ture, especially the stacking of prismatic layers. This follows from the considerable sharpening of the $(10l)$ lines with $l = 2, 3, 5$. Interestingly most of the effect is already shown by introduction of nickel up to an atomic ratio Ni/W = 0.1. Linear dimensions of the WS_2 crystallites in the direction of the c-axis and in the ab plane ("thickness" and "diameter," respectively) were calculated using the formula (9),

$$D = \frac{1.07\lambda}{\beta \cos\theta,}$$

where D is the dimension (Å), λ the wavelength, and β the corrected line width in radians. The results in Table 3 show that nickel increases the sizes of the crystallites and also the $D(ool)/D(hko)$ or thickness/ diameter ratio, thus changing the habit of the WS_2 crystallites. Nickel in alumina-sup-
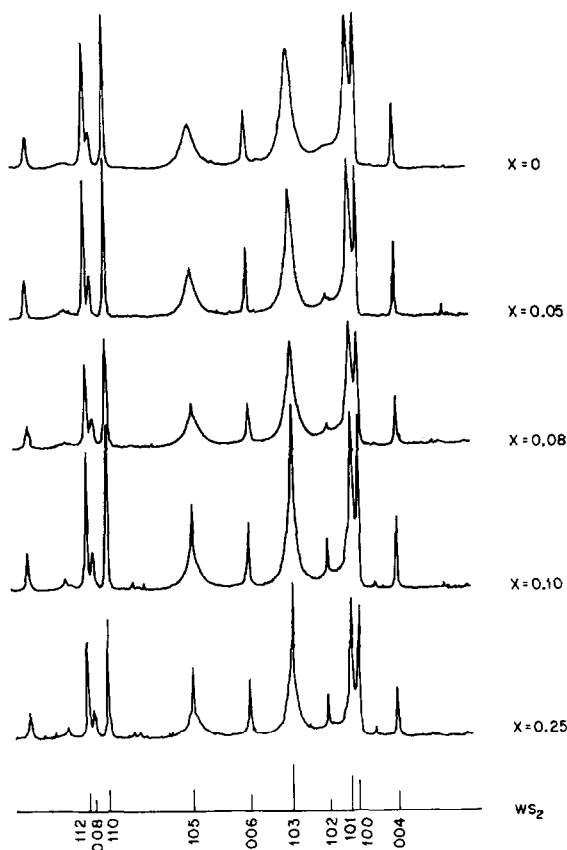

FIG. 5. Densitometer traces of Guinier photographs of tungsten disulfide and nickel–tungsten sulfide: Ni/W atomic ratio indicated with the curves.
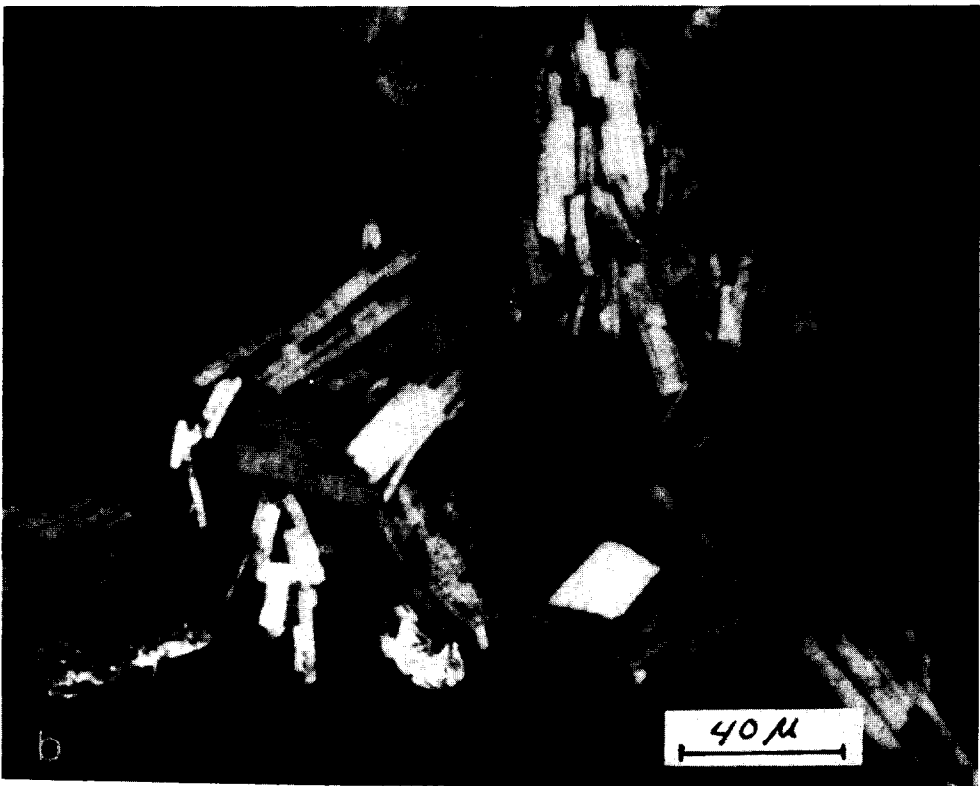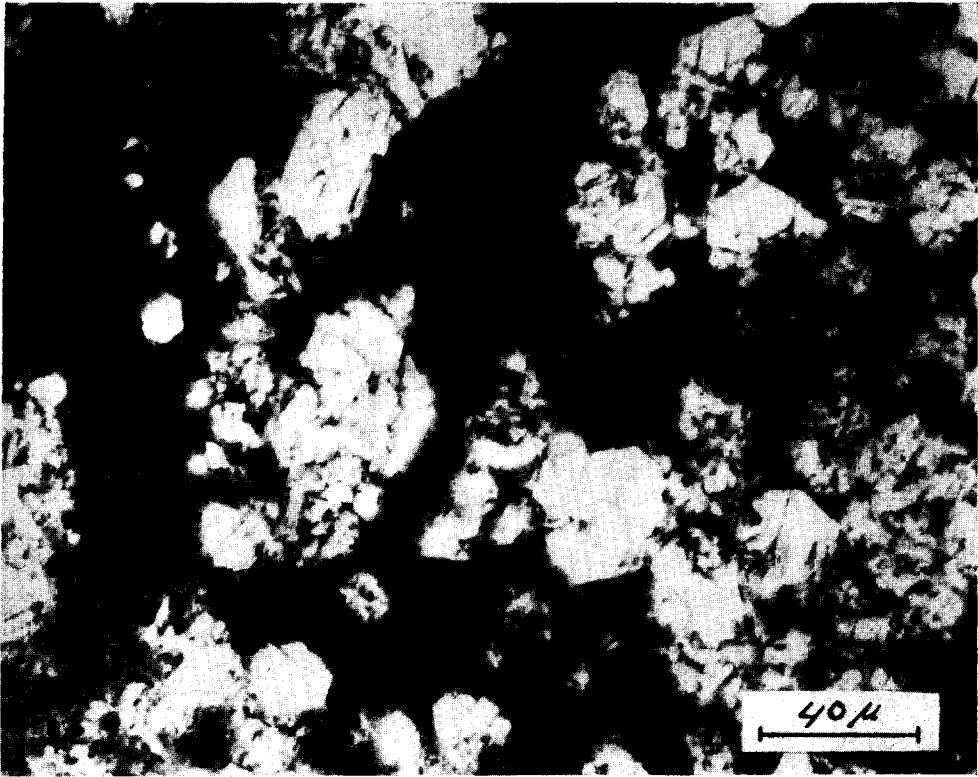
FIG. 6. Micrographs of tungsten disulfide crystals (a) and nickel–tungsten sulfide (b).

248

TABLE 3
EFFECT OF NICKEL ON THE DIMENSIONS OF WS$_2$ CRYSTALLITES

Method	Type of catalyst	Tungsten disulfide			Nickel–tungsten sulfide		
		Height (Å)	Diam (Å)	Ratio	Height (Å)	Diam (Å)	Ratio
X-Ray	Bulk	280	340	0.8	580	490	1.2
	Al$_2$O$_3$-supported	38	56	0.7	51	53	1.0
Microscopy	Bulk	$<10^4$	3.5×10^5	<0.03	2.5–20×10^4	1.5–4×10^5	0.1–0.7

ported WS$_2$ shows much the same effect (Table 3).

Tungsten disulfide, embedded in Bakelite for microscopic investigation, shows many damaged crystals, but the hexagonal sheet-like structure is still apparent (Fig. 6a). The crystals are very thin, generally less than 1 μ, and mechanically very weak. Nickel–tungsten sulfide Ni$_{0.5}$WS$_2$ prepared under the same conditions, but excess nickel removed by iodine transport, shows much thicker and stronger WS$_2$ crystals. The sidefaces of the WS$_2$ plates are easily identified by the optical anisotropy of WS$_2$ (Fig. 6b). The crystals are about 4–15 μ thick. It is evident that the ratio of height to diameter is increased by added nickel (Table 3).

Crystallite sizes measured under the microscope are much larger than those inferred from X-ray line broadening. This may be caused by the crystals being conglomerates, containing perfect order regions separated by low angle and twin boundaries.

The evidence for the incorporation of nickel into WS$_2$ suggests only limited insertion, perhaps to about Ni/W = 0.1, as shown by the fact that the structural effect of nickel is not increased beyond that ratio.

5. STRUCTURE OF WS$_2$ SURFACE SITES, ADSORPTION OF HYDROCARBONS, AND THE ROLE OF NICKEL

It seems rather well established [Refs. (1 and 2), this paper] that tungsten ions in the surface of tungsten disulfide crystals are the active sites in hydrogenation. It therefore appears worth while to discuss the WS$_2$ structure in some more detail.

In Fig. 4, the basal plane consisting of a close-packed sulfur array is shown to provide an easy cleavage plane. To construct a stoichiometric crystallite of small dimensions, it is obviously necessary to place part of the tungsten ions in a partly incomplete sulfur prism. Because of electrostatic interaction and polarization energy terms in the binding energy, it is more favorable to leave sulfur vacancies in the side faces of the sheets than in the basal plane. This is shown by calculations for the similar case of the titanium chlorides (10, 11). The anisotropy of the chemical properties of layer sulfides further supports this view (12).

A model of a small stoichiometric WS$_2$ crystal (Fig. 7), constructed with no vacancies in the basal plane, shows that, along the side face, tungsten ions in 5-coordination appear. At the corners of the sheet, corresponding to edges parallel to the c-axis of the crystal, tungsten ions are present in 4-coordination. Other tungsten coordinations may be present also, but they are too well shielded by sulfur ions, and it is not necessary to take them into account as active sites.

It seems likely that adsorption of the organic species will occur on single sites, as the distances between adjacent sites (3.15 Å for undistorted WS$_2$) and the Van der Waals radius of the sulfur ion (1.8 Å) rule out two-center adsorption. On the basis of parallels in coordination chemistry, a π-adsorption complex is postulated for olefins and aromatics on the tungsten ions. Sandwich complexes of tungsten, molybdenum and chromium with benzene are well known (13, 14), and π-olefinic complexes have also been reported to be stable, even beyond 200°C [Ref. (15)]. In fact, adsorptions of olefins and aromatics on transition metal surfaces are commonly assumed to be of the π-type (16, 17).
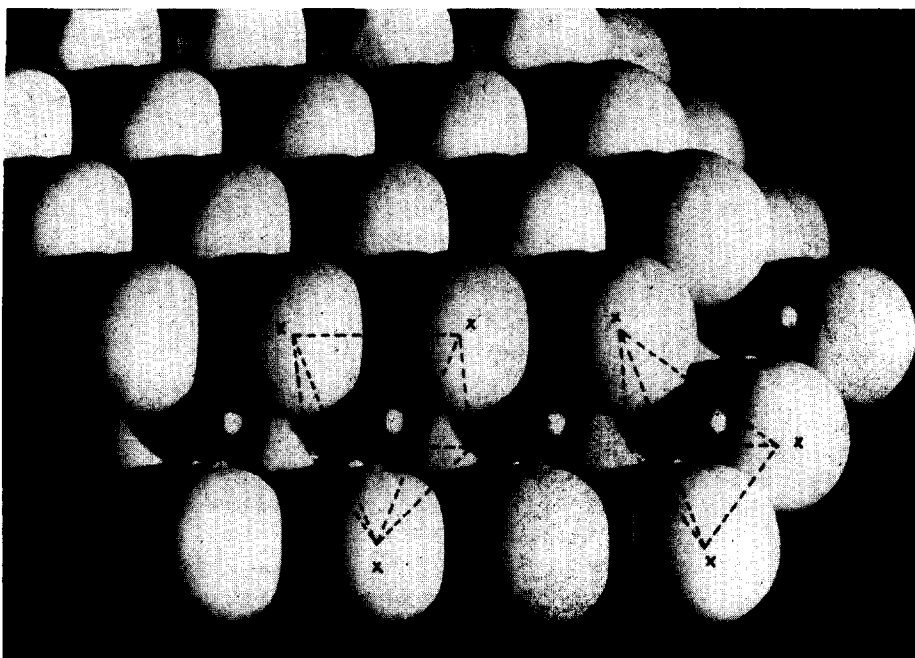
FIG. 7. Model of small WS_2 crystallite (one sandwich): White spheres represent sulfur ions, black balls tungsten ions. Steric hindrance of adsorption is caused by sulfur ions marked by crosses.

In order to act as active hydrogenation sites, it should be stereochemically possible for the two sites discussed above to adsorb cyclohexene or benzene, or both. Little problem seems to arise for the "edge-on" π-adsorption of cyclohexene on either site. For benzene, however, the situation is different. Adsorption as a π-complex, with structure and bonding similar to dibenzene tungsten, would give a distance between the tungsten ion and the benzene C-plane of 3.3 Å for the pentacoordinated tungsten ion, and of 2.6 Å for the tetracoordinated ion. The Van der Waals radii of sulfur ions and the thickness of the benzene ring are used for this calculation. Of course the actual distances may well be somewhat below these values without giving too high repulsive interaction. The value of 3.3 Å rules out adsorption of benzene on the pentacoordinated site, but 2.6 Å, for the tetracoordinated site, is close enough to the corresponding distance in dibenzene tungsten (estimated at 1.8 Å) to allow fairly stable bonding.

Taking into account the ESR evidence

(2) that benzene is hydrogenated on W^{3+} ions, it is considered likely that benzene is hydrogenated via adsorption on a W^{3+} ion in a coordination of four sulfur ions. In the absence of a correlation between cyclohexene hydrogenation activity and the presence of ESR-active tungsten ions, it is possible that cyclohexene is hydrogenated on both W^{3+} and W^{4+} ions in either 4 or 5-coordination of sulfur.

The discussion of the adsorption sites above suggests a ready explanation for the promoter effect of nickel on WS_2. If nickel is inserted between the WS_2 sandwiches, as the evidence in the previous section suggests, it will contribute electrons to the WS_2 hostlattice. This may be concluded from studies of $Na(WS_2)_n$, which showed the electronic structure to be $Na^+(WS_2)_n{}^-$ [Ref. (5)] and also from studies of the compounds $Ni(MeS_2)_n$, with Me = Nb, Ta, of which the electronic structures are $Ni^{2+}(MeS_2)_n{}^{2-}$ [Refs. (7, 18)]. The resulting structure of $Ni(WS_2)_n$, with electrons introduced into the WS_2 layer free to move to W^{4+} ions (Fig. 8), shows clearly how nickel can pro-
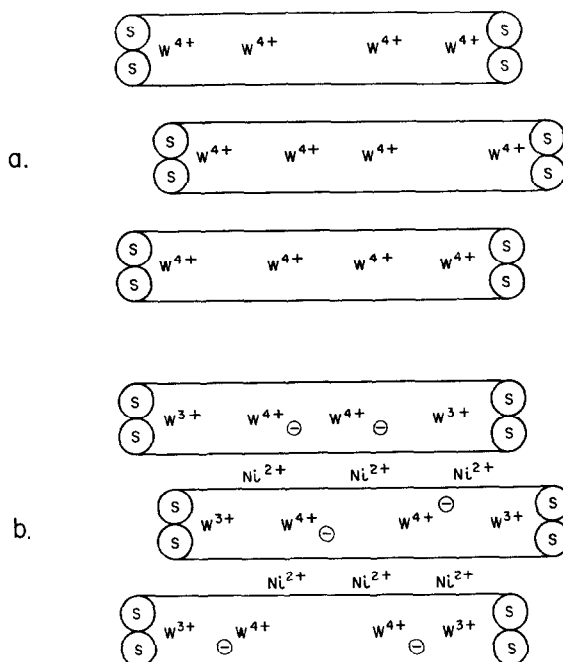
FIG. 8. Schematic of the structure of WS$_2$ layers showing the electronic effect of nickel insertion increasing the number of W^{3+} sites: (a) WS$_2$; (b) Ni$_x$WS$_2$.

mote very effectively the hydrogenation of benzene by increasing the number of active W^{3+} sites.

Although no localized electrons on tungsten ions were found necessary for the cyclohexene hydrogenation it is possible that the increased electron density on the pentacoordinated tungsten ions is favorable for the cyclohexene hydrogenation, leading to the (rather modest) promoter effect of nickel for this reaction. It is noticeable that nickel does not itself act as hydrogenation site. The limited amount of nickel which can be inserted into the WS$_2$ layers explains why the hydrogenation activity is most increased by the first small amount of nickel (Table 2) and does not rise further beyond an atomic ratio Ni/W $\simeq$ 0.1 (Fig. 2).

No zero-valent nickel was found in any of these catalysts, as they were studied by ESR. The hydrogenation activity can not be attributed to free nickel, since addition of nickel beyond Ni/W $\sim$ 0.1 does not increase the activity. The H$_2$S/H$_2$ ratios employed throughout preclude the reduction of Ni$_3$S$_2$ [Ref. (19)].

6. CONCLUSIONS

The present study of hydrogenation on nickel–tungsten sulfide and tungsten disulfide catalysts [Refs. (1, 2), and this paper] has shown the following:

1. Both the hydrogenations of cyclohexene and benzene are first order, indicating that the reaction rate is strongly dependent on the adsorption of the hydrocarbon.

2. The sites active for hydrogenation of these hydrocarbons are sulfur deficient, being blocked by H$_2$S and CS$_2$.

3. The intrinsic activity of the sites in tungsten-disulfide based catalysts is constant, independent of the presence of nickel. This shows that the sites are tungsten ions in the WS$_2$ lattice. Because of energetic considerations, it is probable that the sites are ions at the corners and edges of the tungsten disulfide plates.

4. Sites active in benzene hydrogenation are W^{3+} ions, as shown by ESR.

5. The W^{3+} ion which is the active site for benzene hydrogenation is on stereo-

chemical grounds likely to be coordinated by four sulfur ions.

6. Cyclohexene hydrogenation is shown to proceed on different sites than benzene hydrogenation. It is postulated that, in addition to four coordinated W^{3+} ions, five coordinated and mostly quadrivalent tungsten ions are active sites for this olefin.

7. The hydrogenations of benzene and cyclohexene are postulated to proceed *via* π-bonded adsorption complexes in which the hydrocarbons are bound to tungsten ions in the WS_2 surface.

8. Nickel is inserted into the WS_2 layer structure between adjacent sulfur layers up to a Ni/W ratio of about 0.1. It is likely to be ionized. The promoter effect is due to an increase in the electron concentration in the WS_2 sheets, producing an increased number of active tungsten ions in the surface. The increase in the number of W^{3+} ions has been shown by ESR.

9. Dispersion of the catalyst on an alumina support, as in the BASF catalyst, increases the number of active sites but does not change the intrinsic activity of the sites for benzene or cyclohexene hydrogenation.

10. The hydrogenolysis of carbon disulfide shows the same activation energy on bulk and on alumina-supported nickel–tungsten sulfide. This indicates that the active sites have the same intrinsic activity in both cases. The active sites in tungsten disulfide and in nickel–tungsten sulfide appear to be different for this reaction.

ACKNOWLEDGMENTS

REFERENCES

1. VOORHOEVE, R. J. H., AND STUIVER, J. C. M., *J. Catal.* **23**, 228 (1971).
2. VOORHOEVE, R. J. H., *J. Catal.* **23**, 236 (1971).
3. VOORHOEVE, R. J. H., AND WOLTERS, H. B. M., *Z. Anorg. Allg. Chem.* **376**, 165 (1970).
4. SWANSON, H., GILFRICH, N. T., AND COOK, M. I., *Nat. Bur. Stand. Circ.* **539**, 65 (1958).
5. RUDORFF, W., *Chimia* **19**, 489 (1965).
6. JELLINEK, F., *Ark. Kemi* **20**, 447 (1963).
7. VAN DEN BERG, J. M., AND COSSEE, P., *Inorg. Chim. Acta* **2**, 143 (1968).
8. VAN DEN BERG, J. M., *Inorg. Chim. Acta* **2**, 216 (1968).
9. KLUG, H. P., AND ALEXANDER, L. E., "X-Ray Diffraction Procedures," p. 491 ff. Wiley, New York, 1954.
10. ARLMAN, E. J., *J. Catal.* **3**, 89 (1964).
11. ARLMAN, E. J., *Rec. Trav. Chim. Pays-Bas* **87**, 1217 (1968).
12. THOMAS, J. M., *Advan. Catal. Relat. Subj.* **19**, 293 (1969).
13. FISCHER, E. O., SCHERER, F., AND STAHL, H. O., *Chem. Ber.* **93**, 2065 (1960).
14. DOBSON, G. R., STOLZ, I. W., AND SHELINE, R. K., *Advan. Inorg. Chem. Radiochem.* **8**, 1 (1966).
15. QUINN, H. W., AND TSAI, J. H., *Advan. Inorg. Chem. Radiochem.* **12**, 217 (1969).
16. ROONEY, J. J., *J. Catal.* **2**, 52 (1963).
17. GARNETT, J. L., AND SOLLICH-BAUMGARTNER, W. A., *Advan. Catal. Relat. Subj.* **16**, 95 (1966).
18. ANZENHOFER, K., VAN DEN BERG, J. M., COSSEE, P., AND HELLE, J. N., *J. Phys. Chem. Solids* **31**, 1057 (1970).
19. ROSENQVIST, T., *J. Iron Steel Inst. London* **176**, 37 (1954).